

# Significantly Improved Analytical Sensitivity of Lateral Flow Immunoassays by Using Thermal Contrast\*\*

Zhenpeng Qin, Warren C. W. Chan, David R. Boulware, Taner Akkin, Elissa K. Butler, and John C. Bischof\*

The ability to rapidly identify diseases enables prompt treatment and improves outcomes. This possibility has increased the development and use of rapid point-of-care diagnostic devices that are capable of biomolecular detection in both high-income and resource-limited settings.<sup>[1–4]</sup> Lateral flow assays (LFAs) are inexpensive, simple, portable, and robust,<sup>[5]</sup> thus making LFAs commonplace in medicine, agriculture, and over-the-counter personal use, such as for pregnancy testing. Although the analytical performance of some LFAs are comparable to laboratory-based methods,<sup>[1]</sup> the sensitivity of most LFAs is in the mM to  $\mu$ M range,<sup>[5,6]</sup> which is significantly less sensitive than other molecular techniques such as enzyme-linked immunoassays (ELISAs). As a consequence, LFAs are not particularly useful for detection early in a disease course when there is low level of antigen. Owing to the increasing need for highly sensitive molecular diagnostics, researchers have focused on developing microfluidics,<sup>[1,2]</sup> biobarcodes,<sup>[3,4]</sup> and enzyme-based immunoassay technologies<sup>[7]</sup> to fulfill the need, since these technologies have nM to pM detection sensitivity for protein analysis and can potentially be miniaturized as handheld point-of-care diagnostic devices.<sup>[3]</sup> These emerging technolo-

gies are still early in development and are not yet ready for application by the end user.

With LFAs, antibody-coated gold nanoparticles (GNPs) are moved within a nitrocellulose membrane through capillary action after the strip has been dipped in clinical specimen. When present, the target analyte binds to monoclonal-antibody-coated GNPs. This bound complex stops wicking up the membrane, when capture antibody on the membrane recognizes the antigen-antibody-GNP complex. This recognition event leads to accumulation of GNPs at the test line of the LFA, thereby creating a visually positive test result (Figure 1).

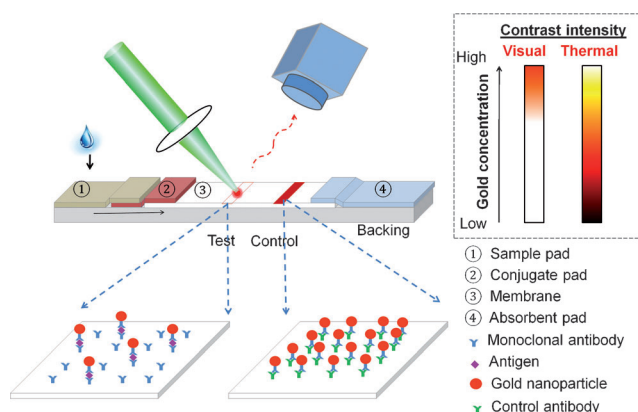


**Figure 1.** Concept of thermal contrast for immunochromatographic lateral flow assays. Monoclonal antibodies conjugated to gold nanoparticles bind the target analyte. This GNP-antibody-antigen complex binds with monoclonal antibodies attached to the dipstick substrate, thereby retaining the GNP in the test region and leading to visible color change (visual contrast) at the test band. At low concentrations of antigen, when there are insufficient bound GNPs for visual contrast, thermal contrast can detect the presence of GNPs in the test band (inset), with a low-cost laser or light-emitting diode (LED; shown in green) and an infrared temperature gun (shown as blue box), which is available over-the-counter. The control band ensures the success of the assay.

GNPs are traditionally used for LFAs, because their size can be designed to easily migrate through the pores of the membrane; GNPs can easily be coated with antibodies; and GNPs have a high molar absorptivity of light and thus produce a deep color that is easily visualized. Herein, we show a low-cost, creative solution to improve sensitivity of LFAs. Metallic nanoparticles generate heat upon optical stimulation.<sup>[8]</sup> This heat generation results from surface plasmons at the metal-dielectric interface during transition from an excited to ground state.<sup>[9]</sup> The amount of heat generated by GNPs can be described by the following equation:<sup>[8,10]</sup>

[\*] Z. Qin, Prof. J. C. Bischof

Department of Mechanical Engineering, University of Minnesota  
111 Church St. SE, Minneapolis, MN 55455 (USA)  
E-mail: bischof@umn.edu

Homepage: <http://me.umn.edu/people/bischof.shtml>

Prof. T. Akkin, Prof. J. C. Bischof

Department of Biomedical Engineering  
University of Minnesota (USA)

Prof. J. C. Bischof

Department of Urology, University of Minnesota (USA)

Prof. D. R. Boulware, E. K. Butler

Department of Medicine, Center for Infectious Disease and Microbiology Translational Research, University of Minnesota (USA)

Prof. W. C. W. Chan

Institute of Biomaterials & Biomedical Engineering & Terrence Donnelly Center for Cellular and Biomolecular Research  
University of Toronto, Toronto, ON (Canada)

[\*\*] This work is supported partially by McKnight Professorship and Minnesota Futures Grant from the University of Minnesota, and NSF/CBET Grant no. 1066343(JCB). D.R.B. is supported by the National Institute of Health, NIAID K23AI073192, and E.B. is supported by NIH NIAID U01AI089244. The authors thank Greg Huan and Vincent Blonigen for the help with the thermal contrast experiment, Neha Shah for the training of GNP synthesis, Robert Hafner and Pingyan Lei for the help with TEM imaging.



Supporting information (including complete experimental methods) for this article is available on the WWW under <http://dx.doi.org/10.1002/anie.201200997>.

$$Q = N Q_{\text{nanop}} = N C_{\text{abs}} I \quad (1)$$

where the total heat generation ( $Q$ ,  $\text{W m}^{-3}$ ) is the combined contribution of single GNP ( $Q_{\text{nanop}}$ ,  $\text{W}$ ), written as the product of GNPs concentration ( $N$ ,  $\text{GNPs m}^{-3}$ ), GNP absorption cross-section ( $C_{\text{abs}}$ ,  $\text{m}^2$ ), and laser intensity ( $I$ ,  $\text{W m}^{-2}$ ). As is now well-known the optical,<sup>[11]</sup> thermal,<sup>[12]</sup> and electrical<sup>[13]</sup> properties of materials change dramatically in the nanoscale. In particular, the enhanced photothermal signature of metal nanoparticles have been utilized for thermal destruction of malignant tumors,<sup>[14–17]</sup> detecting circulating tumor cells,<sup>[18]</sup> photothermal molecule release<sup>[19]</sup> and gene transfection,<sup>[20,21]</sup> enhancing the therapeutic efficiency of chemotherapeutics,<sup>[22]</sup> and for tracking the transport of nanoparticles within cells.<sup>[23]</sup> Herein, we determined whether thermal contrast could improve the analytical sensitivity of existing, commercial LFAs. Our results show a 32-fold improvement in analytical sensitivity when using an FDA-approved LFA for cryptococcal antigen with the potential to increase the sensitivity 10000-fold by engineering the design of the LFA substrate and nanoparticle.

First, we compared the thermal contrast versus visual contrast of GNPs in solution. A series of different concentrations of GNPs were prepared. The GNP solution ( $10 \mu\text{L}$ ) was placed on a microscope slide. For visual analysis, a picture was taken by a digital camera and analyzed later with the software Image J. For thermal analysis, the GNP solution was irradiated with a laser ( $0.5 \text{ W}$ ,  $532 \text{ nm}$ ), and the temperature change was recorded by an infrared camera. Our results show that we can detect down to  $2.5 \times 10^9 \text{ GNPs mL}^{-1}$  of GNPs by using thermal contrast in comparison to  $2.5 \times 10^{11} \text{ GNPs mL}^{-1}$  by visual contrast. This result clearly demonstrates that thermal contrast for detection can improve the overall analytical sensitivity by 100-fold (Figure 2B). We also compared thermal contrast of GNPs with optical density measurement using a standard micro-volume plate reader, the principle of which is widely used in microfluidic ELISA.<sup>[7]</sup> With the same sample volume ( $10 \mu\text{L}$ ), the thermal contrast displayed 50-fold improvement over the optical density measurement (Figure S1 in the Supporting Information). Further improvement in thermal contrast sensitivity may be possible by using higher-powered lasers and/or tuning the laser power for different concentrations of GNPs to extend the dynamic range of thermal contrast.

Next, we assessed the analytical performance of thermal contrast versus colorimetric detection (i.e. visual contrast) using FDA-approved LFAs (Immy, Inc.) for detecting cryptococcal antigen (CrAg). Cryptococcosis is among the leading causes of death among all AIDS-related opportunistic infections and is the most common cause of meningitis in adults in Africa and causes more than 500000 deaths worldwide annually.<sup>[24,25]</sup> Cryptococcal meningitis is classically diagnosed by a combination of culture, India ink, or CrAg testing with semi-quantification by serial twofold dilutions (i.e. CrAg titer, which is defined as the last positive test when performing two-fold serial dilutions). We compared by LFA serial two-fold dilutions of a patient serum specimen with asymptomatic cryptococcal antigenemia,<sup>[26]</sup> positive at 1:32768 titer by latex agglutination (Immy, Inc.). Our results

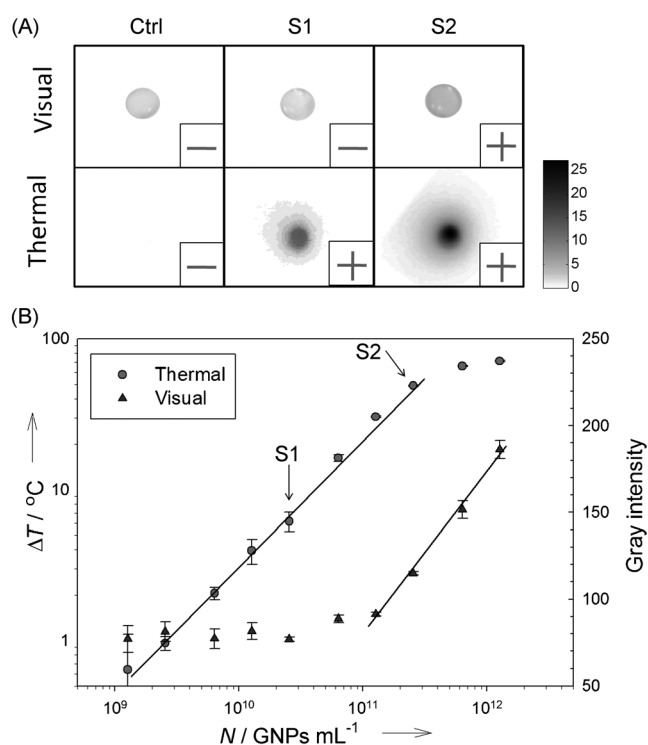


**Figure 2.** Thermal contrast enhances the detection of gold nanoparticle solution. A) Examples of visual and thermal images of GNP solution and pure water (Ctrl). B) Experimental demonstration showing 100-fold increase in the limit of detection with a continuous wave (CW) laser ( $0.5 \text{ W}$ ,  $532 \text{ nm}$  wavelength). With higher laser power, lower concentrations of GNPs can be detected.

show that thermal contrast was indeed more sensitive than colorimetric visual detection on the LFA (Figure 3A). Figure 3B shows thermal contrast produced a 32-fold greater improvement in the analytical sensitivity than colorimetric detection with a log-linear slope up to an equivalent concentration of 1:1024 CrAg titer (S3 in Figure 3B) by latex agglutination ( $R^2 = 0.98$ ). Above this 1:1024 titer, there was a high dose “hook” effect with decreased visual intensity and a plateau of thermal intensity. This effect can be overcome either by changing the dilution of the assay, or by changing the engineering of the assay. We have further validated thermal contrast in 158 clinical cerebral spinal fluid (CSF) samples with known CrAg titers from patients with and without cryptococcus from a published cohort.<sup>[27]</sup> These results show a strong correlation between the traditional (i.e. titer) and the new thermal contrast technique ( $R^2 = 0.88$ , data not shown) without any loss in specificity. In addition, the inter-assay precision of the assay can be improved by standardizing the size of these nanoparticles to decrease the coefficient of variance (Figure S2 in the Supporting Information). For comparison, the median CrAg titer observed in patients with cryptococcal meningitis is often 1:1024 to 1:2048.<sup>[28,29]</sup> However, there is a sub-acute onset over weeks to months. CrAg titers above 1:8 in asymptomatic persons with subclinical disease are predictive of later development of cryptococcal meningitis with 100% sensitivity and 96% specificity despite HIV therapy.<sup>[30]</sup> Serum CrAg screening and preemp-

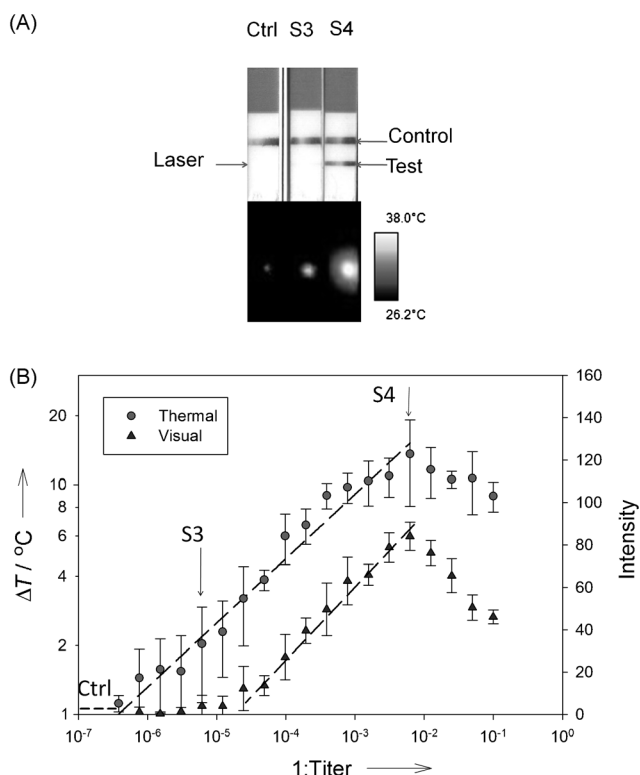


**Figure 3.** Thermal contrast enhances the detection of existing immunochromatographic lateral flow assays for cryptococcal antigen. A) Examples of visual and thermal images of dipsticks used for CrAg diagnosis. B) Quantitative measurement of the thermal and visual detection of LFA at twofold serial dilutions. Thermal contrast (laser power 0.01 W, 532 nm) shows extended dynamic range versus visual contrast. The drop of signal at high concentrations is due to the high dose hook effect inherent with the LFA. The short horizontal dashed line at low concentrations shows background from the control samples (water).

tive antifungal treatment in persons living with advanced AIDS aborts the clinical progression to symptomatic meningitis.<sup>[26]</sup> Noninvasive screening is possible with CrAg being detectable in urine, but urine has 22-fold lower CrAg concentration than blood.<sup>[31]</sup> Thus, improvement in LFA sensitivity by thermal contrast would enable noninvasive screening of asymptomatic persons with AIDS and quantification of CrAg burden to stratify future risk of symptomatic disease.

Finally, we explored how to further improve the analytical sensitivity of LFAs. While spherical gold nanoparticles are conventionally used for LFAs, a new generation of nanoparticle structures has been synthesized with much higher absorption cross-sections than gold nanospheres. These new generation of nanoparticles include gold nanorods,<sup>[17]</sup> nanoshells,<sup>[14]</sup> and gold nanocubes.<sup>[16]</sup> For instance, at the equivalent laser power and nanoparticle concentration, typical nanorods and nanoshells generate 4.6-fold and 36-fold more heat than gold nanospheres, respectively (Figure 4A; with size specified in Figure caption). To eliminate the particle size effect, the absorption cross-section ( $C_{\text{abs}}$ ) is normalized by particle volume ( $V$ ) to give a better assessment of the heat generation capability. When this normalization is used, gold

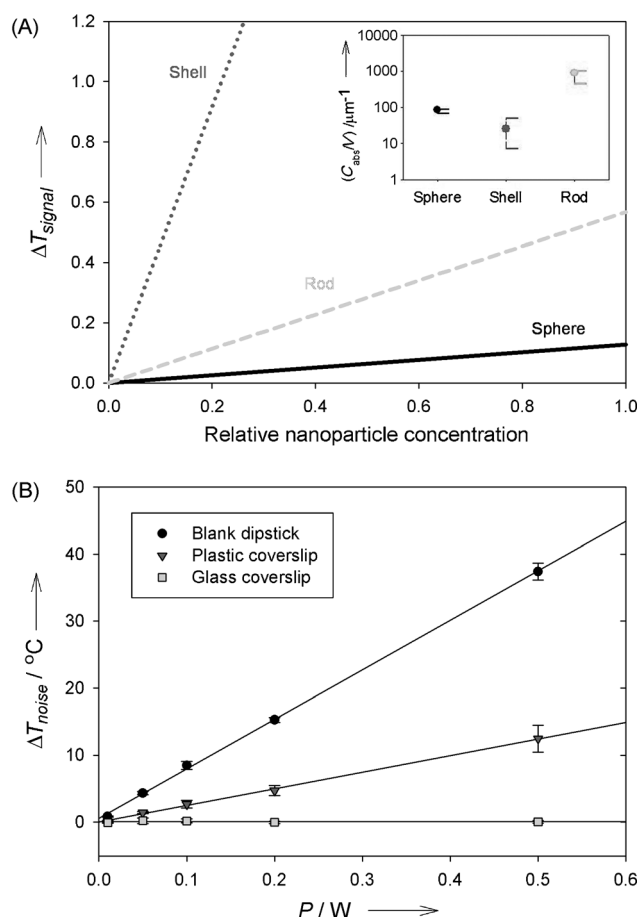


**Figure 4.** Strategies to improve thermal contrast by several orders of magnitude. A) Thermal contrast can be improved by increasing the absorption per nanoparticle. Particle parameters ( $D$  = diameter,  $L$  = length): sphere  $D = 30$  nm, nanorod  $D = 12.7$  nm by  $L = 49.5$  nm, and nanoshell  $D_{\text{core}} = 120$  nm (silica),  $D_{\text{shell}} = 150$  nm (gold). The thermal contrast ( $\Delta T_{\text{signal}}$ ) and nanoparticle concentrations are normalized. Inset shows the typical range of the absorption cross-section per particle volume ( $C_{\text{abs}}/V$ ) as calculated by Jain et al.<sup>[32]</sup> The filled circles indicate the particular particles chosen for the plot. B) Thermal contrast generated by different substrates with varying laser power ( $P$ ). Reduction of the background absorption would: 1) increase the signal-to-noise ratio, and 2) allow the use of higher-intensity laser excitation to increase the sensitivity and dynamic range of the thermal contrast measurement.

nanorods are about one order of magnitude more efficient in heat generation than the gold nanospheres and nanoshells<sup>[8,32]</sup> (Figure 4A inset). Moreover, current LFAs (i.e. thin nitrocellulose membranes with thick backing material) absorb significant amounts of laser energy (at 532 nm), thereby creating background heating or noise (Figure 4B). Thus, use of low-absorbing (i.e. high-transmitting or reflective) backing materials (e.g. glass shown in Figure 2 and plastic used in microfluidic ELISA<sup>[7]</sup>) will allow the use of higher laser intensities ( $I$ ). The combination of higher-absorbing nanoparticles and low-absorbing LFA backing materials should lead to a further improvement in sensitivity. We should be able to produce a 1000-fold increase in thermal contrast by increasing the power density by 100 times (i.e., increase in laser power from 0.01 to 1 W) and using a nanoparticle with

a 10-fold increase in absorption ( $C_{\text{abs}}$ ). Considering this increase in contrast and the 32-fold improvement already shown in cryptococcal LFA (0.01 W laser and spherical GNP), an improvement in the range of four orders of magnitudes is possible.

Aside from the improvement in the analytical sensitivity, these LFAs can also be archived for future analysis. Unlike fluorescence detection, we did not observe any loss of signal through continuous excitation (Figure S3 in the Supporting Information). In fluorescence measurements, organic fluorophores experience photobleaching. In some colorimetric measurements, the dyes may lose their signal over time through photodestruction. When repeating thermal contrast readings at two weeks, the intra-assay reading is nearly identical ( $R^2 = 0.99$ , data not shown). This signal consistency could allow for processing point-of-care LFAs in the field and referral to a central lab to process for thermal contrast readings.

In conclusion, thermal contrast can be used on clinically available LFAs to extend the analytical sensitivity by 32-fold. With further modification of the assay (e.g. light source, nanoparticle absorption, and substrate) a 10000-fold improvement in sensitivity can be expected. This would bring the detection within the range of an ELISA assay. Owing to the low cost and simple handheld nature of LFAs, this technology has applicability in resource-limited and non-laboratory environments with the “disposable LFAs with a reader” model.<sup>[1]</sup> An inexpensive and portable thermal contrast reader could be built and requires only a low-cost laser or light-emitting diode (LED) and infrared temperature gun, which is available over-the-counter, or thermochromic ink that can be printed on paper.<sup>[33]</sup> Thus we conclude that the use of thermal contrast is a promising novel detection mode for improving the analytical sensitivity of biomolecular point-of-care diagnostics and for expanding the use of LFAs.

Received: February 7, 2012

Published online: March 23, 2012

**Keywords:** biosensors · diagnostics · immunoassays · nanoparticles · thermal contrast

- [1] P. Yager, T. Edwards, E. Fu, K. Helton, K. Nelson, M. R. Tam, B. H. Weigl, *Nature* **2006**, *442*, 412.
- [2] A. W. Martinez, S. T. Phillips, G. M. Whitesides, E. Carrilho, *Anal. Chem.* **2010**, *82*, 3.
- [3] J. M. Klostrianec, Q. Xiang, G. A. Farcas, J. A. Lee, A. Rhee, E. I. Lafferty, S. D. Perrault, K. C. Kain, W. C. W. Chan, *Nano Lett.* **2007**, *7*, 2812.
- [4] J.-M. Nam, C. S. Thaxton, C. A. Mirkin, *Science* **2003**, *301*, 1884.
- [5] G. Posthuma-Trumpie, J. Korf, A. van Amerongen, *Anal. Bioanal. Chem.* **2009**, *393*, 569.
- [6] J. Liu, D. Mazumdar, Y. Lu, *Angew. Chem.* **2006**, *118*, 8123; *Angew. Chem. Int. Ed.* **2006**, *45*, 7955.
- [7] C. D. Chin, T. Laksanasopin, Y. K. Cheung, D. Steinmiller, V. Linder, H. Parsa, J. Wang, H. Moore, R. Rouse, G. Umvilighozo, *Nat. Med.* **2011**, *17*, 1015.
- [8] A. O. Govorov, H. H. Richardson, *Nano Today* **2007**, *2*, 30.
- [9] S. A. Maier, *Plasmonics: fundamentals and applications*, Springer, Heidelberg, **2007**.
- [10] Z. Qin, J. C. Bischof, *Chem. Soc. Rev.* **2012**, *41*, 1191.
- [11] K. L. Kelly, E. Coronado, L. L. Zhao, G. C. Schatz, *J. Phys. Chem. B* **2003**, *107*, 668.
- [12] S. Shen, A. Henry, J. Tong, R. Zheng, G. Chen, *Nat. Nanotechnol.* **2010**, *5*, 251.
- [13] H. Dai, E. W. Wong, C. M. Lieber, *Science* **1996**, *272*, 523.
- [14] L. R. Hirsch, R. J. Stafford, J. A. Bankson, S. R. Sershen, B. Rivera, R. E. Price, J. D. Hazle, N. J. Halas, J. L. West, *Proc. Natl. Acad. Sci. USA* **2003**, *100*, 13549.
- [15] G. von Maltzahn, J. H. Park, A. Agrawal, N. K. Bandaru, S. K. Das, M. J. Sailor, S. N. Bhatia, *Cancer Res.* **2009**, *69*, 3892.
- [16] J. Chen, D. Wang, J. Xi, L. Au, A. Siekkinen, A. Warsen, Z.-Y. Li, H. Zhang, Y. Xia, X. Li, *Nano Lett.* **2007**, *7*, 1318.
- [17] E. C. Dreaden, A. M. Alkilany, X. Huang, C. J. Murphy, M. A. El-Sayed, *Chem. Soc. Rev.* **2012**, *41*, 2740.
- [18] E. Galanzha, E. Shashkov, T. Kelly, J. Kim, L. Yang, V. Zharov, *Nat. Nanotechnol.* **2009**, *4*, 855.
- [19] A. B. S. Bakhtiari, D. Hsiao, G. Jin, B. D. Gates, N. R. Branda, *Angew. Chem.* **2009**, *121*, 4230; *Angew. Chem. Int. Ed.* **2009**, *48*, 4166.
- [20] G. B. Braun, A. Pallaoro, G. Wu, D. Missirlis, J. A. Zasadzinski, M. Tirrell, N. O. Reich, *ACS Nano* **2009**, *3*, 2007.
- [21] W. Lu, G. Zhang, R. Zhang, L. G. Flores, Q. Huang, J. G. Gelovani, C. Li, *Cancer Res.* **2010**, *70*, 3177.
- [22] T. S. Hauck, T. L. Jennings, T. Yatsenko, J. C. Kumaradas, W. C. W. Chan, *Adv. Mater.* **2008**, *20*, 3832.
- [23] C. Leduc, J.-M. Jung, R. R. Carney, F. Stellacci, B. Lounis, *ACS Nano* **2011**, *5*, 2587.
- [24] B. J. Park, K. A. Wannmuehler, B. J. Marston, N. Govender, P. G. Pappas, T. M. Chiller, *AIDS* **2009**, *23*, 525.
- [25] J. N. Jarvis, G. Meintjes, A. Williams, Y. Brown, T. Crede, T. S. Harrison, *BMC Infect. Dis.* **2010**, *10*, 67.
- [26] D. B. Meyra, Y. C. Manabe, B. Castelnuovo, B. A. Cook, A. M. Elbireer, A. Kambugu, M. R. Kamya, P. R. Bohjanen, D. R. Boulware, *Clin. Infect. Dis.* **2010**, *51*, 448.
- [27] D. R. Boulware, D. B. Meyra, T. L. Bergemann, D. L. Wiesner, J. Rhein, A. Musubire, S. J. Lee, A. Kambugu, E. N. Janoff, P. R. Bohjanen, *PLoS Med.* **2010**, *7*, e1000384.
- [28] D. R. Boulware, S. C. Bonham, D. B. Meyra, D. L. Wiesner, G. S. Park, A. Kambugu, E. N. Janoff, P. R. Bohjanen, *J. Infect. Dis.* **2010**, *202*, 962.
- [29] T. Bicanic, G. Meintjes, K. Rebe, A. Williams, A. Loyse, R. Wood, M. Hayes, S. Jaffar, T. Harrison, *J. Acquired Immune Defic. Syndr.* **2009**, *51*, 130.
- [30] J. N. Jarvis, S. D. Lawn, M. Vogt, N. Bangani, R. Wood, T. S. Harrison, *Clin. Infect. Dis.* **2009**, *48*, 856.
- [31] J. N. Jarvis, A. Percival, S. Bauman, J. Pelfrey, G. Meintjes, G. N. Williams, N. Longley, T. S. Harrison, T. R. Kozel, *Clin. Infect. Dis.* **2011**, *53*, 1019.
- [32] P. Jain, K. Lee, I. El-Sayed, M. El-Sayed, *J. Phys. Chem. B* **2006**, *110*, 7238.
- [33] A. C. Siegel, S. T. Phillips, B. J. Wiley, G. M. Whitesides, *Lab Chip* **2009**, *9*, 2775.